Pithoragarh District Uttarakhand

by Krish Yadav

Submission date: 10-Jun-2026 10:54AM (UTC+0530)
Submission ID: 2980277697
File name: Krish_Yadav_Thesis.pdf (2.22M)
Word count: 12022
Character count: 63070

CHAPTER 1

INTRODUCTION

1.1 General

Landslides are a significant geo-hazard worldwide, and the Himalayan region is responsible for a large share of global landslide occurrences. The region is characterized by geological conditions, complex topography, and intense rainfall, along with seismic activity, and increasing human interventions such as road construction, excavation, and land-use change. Besides, natural triggers such as earthquakes, glacier retreat, and extreme precipitation events also increase the instability of slopes. A recent study shows that climate change has increased the frequency and scale of landslides, thus magnifying their effects on fragile mountain ecosystems and human settlements.

Landslide Susceptibility Mapping (LSM) is a technique that involves the use of thematic layers that depict various landslide causative factors, such as slope, geology, and hydrology, to recognize landslide-prone areas. In mountainous regions like the Himalayas where landslides happen quite often due to the complex topography and heavy precipitation, LSM plays a significant role in disaster management and land-use planning.

1.2 Landslides

A landslide is defined as the movement of a mass of rock, debris, or earth down a slope. Landslides occur as a result of changes in slope stability as a result of natural or man-made factors. The Himalayan terrain, owing to its young and tectonically active geology, steep gradients, and susceptibility to intense monsoonal precipitation, is among the most landslide-prone regions in the world.

The region is characterized by geological conditions, complex topography, and intense rainfall, along with seismic activity and increasing human interventions such as road construction, excavation, and land-use change. Natural triggers such as earthquakes, glacier

retreat, and extreme precipitation events also increase the instability of slopes. Climate change has further intensified the frequency and scale of landslide events, magnifying their effects on fragile mountain ecosystems and human settlements. Therefore, it is crucial to comprehend the physical processes of landslides and map the areas at risk for efficiently managing hazards and promoting sustainable development in mountain regions.

1.3 Problem statement

The rugged Himalayan terrain of Pithoragarh district, with elevations around 1,627 m, steep slopes, pronounced relief, and deeply incised valleys, creates inherently high landslide susceptibility. Heavy monsoon rains, river erosion, snowmelt, and anthropogenic activities such as road construction have further destabilized these slopes over recent decades.

Despite the recurring nature of landslide disasters in the district, there is an absence of a comprehensive and spatially explicit susceptibility framework that integrates multiple geo-environmental conditioning factors. Existing hazard assessments are often limited in spatial resolution or methodological rigor, which hampers effective disaster risk reduction, infrastructure planning, and land-use management. This study therefore addresses the critical gap by generating reliable Landslide Susceptibility Maps (LSM) using a combination of statistical and multi-criteria decision-making approaches to support evidence-based planning in the region.

1.4 Landslide History of Pithoragarh District

Pithoragarh district has experienced numerous catastrophic landslides over the past few decades, causing significant loss of life and property. Heavy monsoonal rainfall on 18 August 1998 destabilized the slopes above Malpa village, sending a massive debris flow through the settlement and killing over 200 inhabitants. Over a decade later, in August 2009, saturated hillsides collapsed near Kuity town along the Berinag–Munsiyari corridor, burying the villages of Jhakhla and Lah entirely and claiming 43 lives. Both episodes reflect the deadly and recurring nature of rainfall-triggered slope failures across this Himalayan terrain.

During the monsoon of 2016, several debris flows and landslides affected the villages of Didihat, Bastari, and Naulra, causing 21 fatalities within the district. The high susceptibility

of the region to landslides is largely attributed to its proximity to the Main Central Thrust zone, which makes it seismically active and geomorphologically unstable. More recently, intense rainfall on 25 September 2022 triggered fresh landslide events in the district. Subsequently, on 9 October 2022, another rainfall-induced landslide resulted in the temporary closure of the Tanakpur–Pithoragarh highway, further highlighting the ongoing landslide risk in the region.

1.5 Objectives of Study

The primary objective of this study is to prepare and compare landslide susceptibility maps of Pithoragarh district using multiple approaches. The specific objectives of this study are as follows:

- To prepare a comprehensive landslide inventory for Pithoragarh district using the Bhukosh GSI Inventory, supplemented by published literature and field verification.
- To prepare a comprehensive spatial database of ten key landslide conditioning factors relevant to the study area.
- To assess landslide susceptibility by implementing FR, SE, and AHP modelling approaches and producing corresponding susceptibility maps.
- To examine the predictive capability and reliability of the developed models using AUC–ROC analysis and comparative validation based on success-rate and prediction-rate curves.
- To provide a reliable scientific basis for disaster risk reduction, resilient infrastructure planning, and evidence-based land-use management in Pithoragarh district.

CHAPTER 2

LITERATURE WORK

2.1 Literature Review

Yadav, J., Dash, R.K. & Kanungo, D.P (2025) Sapatial prediction of landslides in pithoragarh district, kumaon Himalaya, India. The authors produced LSZ maps for Pithoragarh district based on FR, IV, and WOE models with several landslide inventory points and thirteen conditioning factors. Nearly 31.93% and 37.84 percent of the district is located in high susceptibility zones. The IV model scored the highest with an AUC of 0.758 because of its logarithmic weighting principle. It is suggested that further research involve machine learning for detecting the nonlinear relationships between the factors. Also, they should not make exclusive use of a landslide inventory formed only on historical events since the changing terrain may invalidate it in parts. The benefit of the approach is deriving weights in a transparent manner; the drawback is completely ignoring the subsurface geotechnical parameters.

Shawez, M., Kumar, S., Gupta, V., Kumar, P., and Rawat, G. (2025) Regarding landslide distribution in Darma Valley, it is pretty clear from the proof that the main driving factors are tectonic activities and erosion potential. The tectonic hotspots can be marked by the high stream-length gradient indices and the low valley-floor width-to-height ratios. The use of multivariate statistics allows the exact determination of erosion susceptible sub-basins, which is among the merits. On the other hand, a downside is the lack of deep lithological parameter consideration in statistical models. Results from the study focus on hazard mitigation in the Higher Himalayan regions. On the other hand, the investigation should be reminded of the rain-shadow impacts in the Tethyan areas, where, in fact, it is the weak lithology that is the main reason for landslides, not the precipitation.

Vardhan, P., Kumar, R. & Kaur, S (2025) A The effectiveness of the AHP and SVM methodologies in delineating landslide susceptibility zones was evaluated through a comparative study conducted in the Pithoragarh district. Results reveal that SVM is more accurate in predicting landslides (AUC=0.889), localizing 56% of landslides within the

highest risk areas. These methods are less subjective because of the use of correlation-adjusted weighting and easier multi-source data integration. On the other hand, disadvantages include SVM's reliance on very good quality data to be effective. Reviewers should consider quantitative machine learning as the main method for hazard zonation as this is more objective. On the other hand, they should not fully depend on heuristic AHP models if there are sufficient landslide data obtained for their training.

Khouzani, A.H., Singha, C., Moghimi, A., et al. (2025) present a hybrid ensemble approach (XGB-RFE) for predicting landslide susceptibility and vulnerability of infrastructure in Uttarakhand. The results show very high accuracy of prediction (AUC=0.996) and it is identified that about 30% of the buildings are located in very high-risk areas. Some of the advantages are that it is possible to perform modeling according to the different types of landslides (soil, debris, rock), and the use of recursive feature elimination to select the best variables such as slope and distance to the road. On the contrary, the disadvantages are that some ensemble variants may be too "liberal" in identifying risks. Probably the most important point in reviews should be the incorporation of vulnerability to the building scale. On the other hand, they should avoid treating all landslide types as the same since they result from different geomechanical processes and require separate modelling.

Singh, S., Nayak, N.P., Aggarwal, A., et al. (2025) One of the articles discussed a landslide vulnerability assessment in Chamoli district with the help of the latest technologies in the field of remote sensing and geotechnical investigations. The results showed that a multi-class index overlay and a hybrid machine learning approach (e.g., CNN-LSTM) can accurately predict the hazard scenario. The positive side is that the method can be used extensively to monitor active geological zones and also routes frequently used by the pilgrims as there is a heavy presence of infrastructure in the latter case. On the other hand, drawbacks from the perspective of a historical data lack and a poor connectivity which is rendering the systematic assessments almost impossible going forward.

Chauhan, V., Gupta, L. & Dixit, J. (2025) In this work they used bivariate, multi-criteria decision-making methods and machine learning techniques to map landslides susceptibility

zones in the state of Uttarakhand. The results reveal that 18.47% area of the state comes under landslides high risk zones which are mainly spread in the districts of Uttarkashi, Chamoli and Pithoragarh. The study is among a handful of publications in which geomorphons, a typology of terrain feature, are used for terrain characterization and Random Forest and XGBoost algorithms that are known for their excellent predictive performances have been employed here (AUC > 90%). On the other handeven though the paper addresses the shortcomings of Shannon Entropy and Fuzzy-AHP models, these two are still the worst performing models included in the comparative analysis. The reviews should chiefly highlight powerful machine learning methods as relevant tools for regional planning whereas, they must not recommend the use of linear models for highly complex Himalayan terrains.

Vashistha, A., Joshi, S. & Siva Subramanian, S. (2025) Scenario-based probabilistic risk assessment of earthquake-induced landslides in Uttarakhand. describe a scenario-based probabilistic risk assessment of earthquake-induced landslides in Uttarakhand. Results indicate that seismic scenarios have a major impact on increasing landslide-susceptible areas in these scenarios compared to static conditions, with Rudraprayag as the most exposed district. The main advantage is the combination of Probabilistic Seismic Hazard Assessment (PSHA) with bivariate statistics for hazard quantification at the district level. On the other hand, a main disadvantage is the lack of data on high-resolution fault geometries. Reviews should give top priority to earthquake-induced hazards and risk in regional planning. On the contrary, they should not forget the decisive role of transient ground motion.

Khatun, S., Saha, A., Gogoi, P., Saha, S., Sarkar, R. (2024) Evaluated landslide-prone areas within Bageshwar district using a combination of statistical analyses and machine learning models. The convectional rainfall in Bageshwar district causes landslides which lead to environmental and socio-economic damages. The study used ANN-based and LR-based models for mapping landslide vulnerability by incorporating various factors such as slope, rainfall, land use, and geomorphological parameters. Socio-economic indicators were population, literacy, and infrastructure. The results show that about 9.15% (with ANN) and 7.39% (with LR) of the area are considered highly vulnerable. The model validation with ROC curves shows that the ANN with AUC 84.06% has a higher accuracy than LR with

AUC 75.79%, which results in effective planning and risk mitigation strategies.

Bhardwaj, D., Sarkar, R. (2024) Investigate Frequency Ratio (FR) and Shannon Entropy (SE) methodologies for LSM in Chamoli. Results reveal that the FR model (AUC=0.883) is only marginally more accurate than SE (AUC=0.877) in terms of prediction. One of the benefits is the unbiased integration of thirteen landslide causative factors, including TWI and proximity to roads, without the intervention of experts. On the other hand, the main drawback is that the complex nature of landslides limits prediction to less than 100% accuracy. It is only right to focus on disaster-resilient infrastructure in the reviews. However, the potential for increased reliability through higher-resolution LiDAR data should not be overlooked.

Mallick, Alkahtani, M., Hang, H.T. et al. (2024) The objective of this research paper is to BNP a neural network model (Deep Neural Network-DNN, Evolutionary Neural Network-ENC, and Artificial Neural Network-ANN) by Bayesian optimization technique for landslide susceptibility mapping while SHAP integration has been done for model interpretability as well. The DNN model has been verified against other models and the factors namely elevation, built-up land, low vegetation, specific aspects, shallow soil, high rainfall, lineament density, and road proximity have been identified as the key factors contributing to landslide susceptibility. First, it is good at making reliable predictions; second, it is interpretable. The limitation of the present work is the landslide inventory not having temporal data.

Amol Sharma, Chander Prakash (2023) The research indicates that the construction of roads results in a 2.67-4.17% increase in landslide susceptibility, highlighting the importance of better planning. To handle the problem, it is suggested that the Shannon Entropy model (83-86% accuracy) be used. However, this can be a situation where improper or inadequately planned construction might lead to increasing the risk. The main factors are drainage, TWI, NDVI waterbodies, and proximity to roads. Pros include the GIS-based statistical modeling for powerful analysis and cons include that improper construction can significantly increase the risk of landslides. In the future, large scale landslide inventories and extensive field validation will be necessary for studies in this area.

Ramiz, M., Siddiqui, M.A., Salman, M.S. et al. (2023) The research uses AHP-MCDM for

landslide susceptibility mapping along Rishikesh, Badrinath highway resulting in 0.81 AUC. Post-usage revealed that 27% falls under high susceptibility thereby assisting disaster planning. The main benefits were factor weighting with high precision, the use of GIS for the recognition of susceptibility zones, and a comprehensive analysis. However, it also indicated that regular and detailed evaluations are essential, as increasing human-induced disturbances, particularly those associated with highway construction, pose significant landslide-related challenges. although the destructiveness of landslides is their inherent nature, accurate data are necessary to ensure model reliability.

Sangeeta, Maheshwari, B.K. (2022) Using integrated AHP and RFR along with ten conditioning parameters including seismicity, assessed landslide susceptibility and social vulnerability in Pithoragarh, Kumaun Himalaya. The predictive capability of the LSZ map was demonstrated by AUC values of 0.77 and 0.76. Notably, the high and very high susceptibility categories occupied 34% of the total area yet comprised 73% of the observed landslide locations. the study is expected to combine physical vulnerability with social indicators. Besides this, it should not treat all landslide types as the same. Reduced subjectivity through the integration of the methods is an advantage; however, the lack of geotechnical ground-truth validation is a disadvantage.

Das, S., Sarkar, S. & Kanungo, D.P. (2022) The article basically performs a review of major LSZ mapping trends carried out in the Indian Himalaya during a decade of 2010-2020, stressing the region's extreme vulnerability. Findings mainly highlight the usefulness of LSZ in assessing vulnerability and predicting the future scenarios. Besides, implementation of remote sensing and geographic information system techniques through visual interpretation methods for disaster mitigation at very low costs is more advantages. On the other hand, making decisions based on loosely formalized criteria and unreflected practices is something that should definitely be avoided.

Dam et al. (2022) The research focused on assessing the applicability of two widely used bivariate statistical models, SE and WOE, in identifying landslide-susceptible zones within the Pithoragarh district of Uttarakhand, India. A tectonically disturbed and highly landslide-prone Himalayan region. Using a historical inventory of 91 landslide events compiled from

the Geological Survey of India and Google Earth imagery, the study employed ten conditioning factors — slope degree, aspect, curvature, elevation, land cover, slope-forming materials, geomorphology, distance to rivers, distance to roads, and overburden depth — derived from Aster DEM, GSI reports, and Google Earth data processed through GIS software. The dataset was split 70:30 for training and validation, and based on AUC validation, the WOE model showed enhanced predictive efficiency over the SE model, attaining accuracy values of 68.75% and 52.17%, respectively. Indicating moderate and weak predictive accuracy respectively. Key landslide-influencing factors identified included steep slopes (41.57°–75.19°), west-facing aspects, concave curvature, elevations between 900–1,100 m, quarry land cover, and "Cherty Quartzite with Epidiorite Dykes" as the dominant slope-forming material. Although both models are simpler and less accurate than machine learning approaches such as Naïve Bayes (AUC = 0.873) and Multilayer Perceptron (AUC = 0.864). The authors concluded that the WOE model is better suited for identifying landslide-susceptible zones, highlighting its potential contribution to regional planning and disaster mitigation initiatives and recommended future integration of machine learning methods for improved predictive performance.

2.2 Research Gap Identification

After conducting a comprehensive review of studies based on landslide susceptibility mapping, particularly those involving FR, SE and AHP the following research gaps have been identified:

- Existing studies have not simultaneously evaluated the performance of FR, SE, and AHP approaches for landslide susceptibility assessment in the Pithoragarh district under the same methodological conditions. This limits grasp of how each model performs relatively to each other while experiencing the same geo-environmental conditions.
- Terrain Ruggedness Index (TRI) and Hillshade have seldom been considered as little factors by the researchers for susceptibility studies in Pithoragarh district so their help in landslide susceptibility zonation remains an open question.
- Even though bivariate statistical models like FR and SE have been used in other districts of Uttarakhand, their validation separately through AUC-ROC curves and direct comparison with the expert-based AHP model has not been specifically done.

CHAPTER 3

METHDOLOGY

3.1 Study Area

Pithoragarh District is located in the Kumaon Himalayan region of Uttarakhand, northern India, the boundaries of which extend roughly between 29°34′48″ N latitude and 80°30′12″ E longitude (see Figure 1). The district has a rugged mountainous topography with an area of about 7,217.7 km² and is characterized by the presence of steep slopes, deep valleys, and narrow gorges.

The region's geomorphology is primarily shaped by a vast drainage network linked to the Ganga river system and its major tributaries, viz., the Kali, Dhauliganga, Goriganga, Girthi, Sarju, Keogad, Kutiyangti, Dharam Ganga, and Ramganga rivers, which run through and form the boundaries of the district. Kali River is the main drainage system among them as it flows through very steep valleys. The overall length of the rivers and streams in the district is around 1,358.99 km.

Pithoragarh shares its boundaries with the districts of Almora, Champawat, Bageshwar, and Chamoli, all of which exhibit similar rugged Himalayan topography. The region has an average elevation of around 1,627 m above mean sea level, with significant variations across the district.

The regional geology is represented by a complex sequence of Garhwal Group lithologies, including shale, slate, phyllite, quartzite, dolomite, limestone, magnesite, calc-slate, and metavolcanic rocks, together with granitoid formations of the Almora Crystalline Group that contribute significantly to the area's geological composition.These rocks have been deformed by the major thrusts and fault systems, as reported by the Geological Survey of India (GSI). Landslide issues are frequently reported in road cuts and on river valley slopes that are steep, which is clear from satellite images and geological maps.

The district was chosen as the study area of the present work because it is highly susceptible to landslides that are mainly caused by faulting and folding due to active tectonics,

weathering, and heavy rainfall, as well as increasing human activities, especially the construction of roads and infrastructures. The area is situated in Seismic Zone V, which means that it has a very high earthquake hazard potential.

The climatic characteristics of Pithoragarh are strongly influenced by elevation, resulting in substantial spatial variability across the district. Humid subtropical conditions dominate the lower regions, while the higher altitudes are associated with temperate and alpine climates. The district undergoes four distinct seasonal phases, namely summer, monsoon, winter, and a transitional period. winter temperatures often fall below 0 °C at higher elevations, while summer temperatures in lower valleys may reach 40–45 °C. Frequent historical landslide occurrences in the district highlight the need for systematic landslide susceptibility assessment to support effective hazard management and sustainable regional development.

The monsoon season, which typically extends from June to September, is the most critical period with respect to landslide triggering in the district. During this period, the district receives the majority of its annual rainfall, with mean annual precipitation ranging from approximately 1,000 mm in the drier rain-shadow zones to over 2,000 mm in the more exposed southern and western slopes. Intense and prolonged rainfall events during this season are widely recognized as the primary triggering mechanism for both shallow debris slides and deep-seated rotational landslides across the district. The combination of high precipitation intensity, deeply weathered and fractured rock masses, and steep slope gradients creates conditions that are particularly favorable for slope instability. Several nationally and state highways passing through the district, including the route connecting to the Dharchula and Munsiyari sub-divisions, are regularly disrupted during the monsoon season due to landslide activity, causing significant economic losses and isolating remote communities. The district administration and the State Disaster Management Authority have recorded numerous fatalities and property damages linked to landslide events over the past two decades, further underscoring the urgency of producing reliable susceptibility maps that can inform land use planning, infrastructure development, and early warning system design for the region.

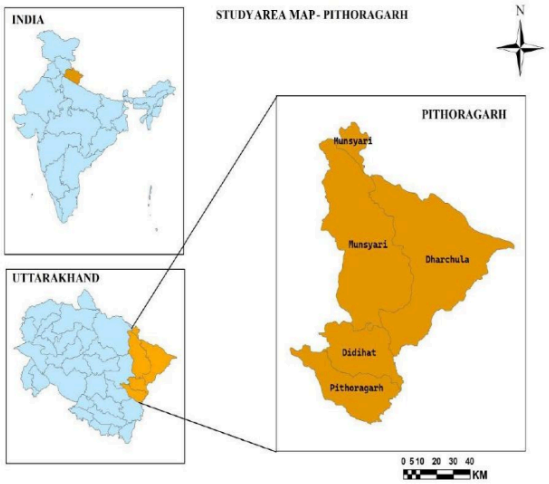

Fig. 1. Study Area – Pithoragarh

3.2 Landslide Inventory Map

Landslide Inventory map showing the spatial distribution of historical landslide events in Pithoragarh District, Uttarakhand. The landslide inventory was obtained from secondary data sources, mainly as polygon and points shapefile from Bhukosh (Government of India) which is a national repository for landslide information These data give a trusted record of previous events and form subject data for validate the model.

In total, 366 landslide locations were compiled covering the entire study area. This landslide inventory is considered of paramount importance for the subsequent landslide susceptibility analysis. To be specific, following the common practice, the inventory allowed for both model validation and training; in this case, 70% of the initial inventory was used as training data, while the rest was used to assess the model performance. It should be added that the

inventory facilitated elaborating on the spatial patterns of historical landslide occurrences concerning the pre-selected topographical, geological, and hydrological conditioning factors. Moreover, the inventory enabled the process of identifying and mapping landslide-prone zones, which were done based on the FR method.

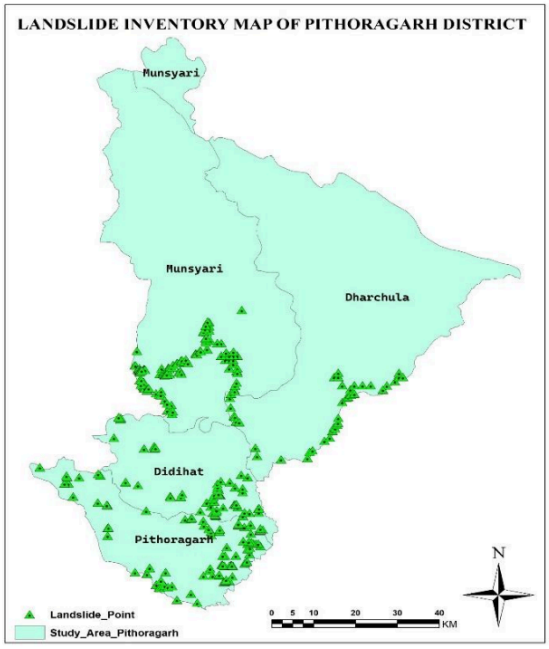

Fig. 2 Landslide Inventory Map

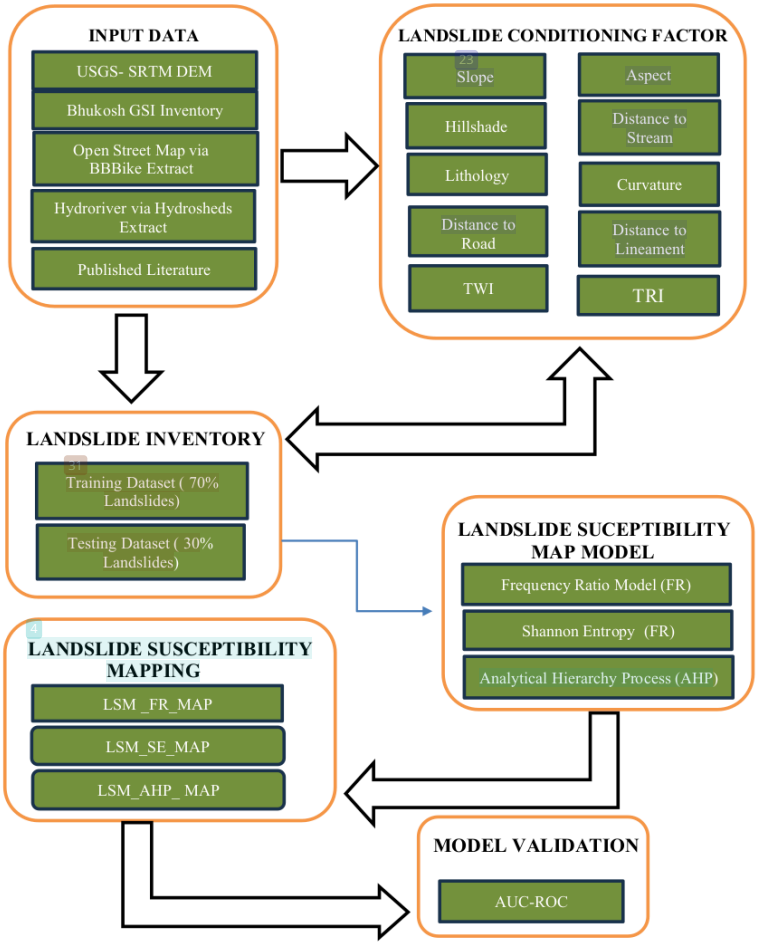

Fig. 3. Methodological Flowchart

TABLE 1. DATA SOURCES FOR THEMATIC MAPS

THEMATIC MAP	DATA SOURCE
INDIAN MAP	https://www.indianremotesensing.com/2017/01/Download-India-shapefile-with-kashmir.html
DISTANCE TO ROAD	https://extract.bbbike.org/
LANDSLIDE POINTS AND DISTANCE TO LINEAMENT	https://bhukosh.gsi.gov.in/Bhukosh/Public
DISTRICT AND SUB-DISTRICT MAPS	https://esriindia1.maps.arcgis.com/home/item.html?id=b89de19cafb94ea38552a55eb5b2d13d
SLOPE, ASPECT, CURVATURE, HILLSHADE	https://earthexplorer.usgs.gov/
DISTANCE TO STREAM	https://www.hydrosheds.org/products/hydrorivers#downloads
LITHOLOGY	https://certmapper.cr.usgs.gov/data/apps/world-maps/
TWI AND TRI	https://opentopography.org/

3.3 Landslide Conditioning Factor

3.3.1 Slope

Besides, the slope angle, which is an index showing the degree of surface slope to the horizontal direction, was generated from the Digital Elevation Model using Spatial Analyst surface tools in ArcGIS. It is also a factor that controls the tendency of surface runoff and shear stresses; hence, it has a great impact on slope instability and the occurrence of landslides. The slope layer was categorized into five groups; 0°–9°, 17°–27°, 27°–37°, 37°–47°, 47-88° to measure the effect on the occurrences of landslides.

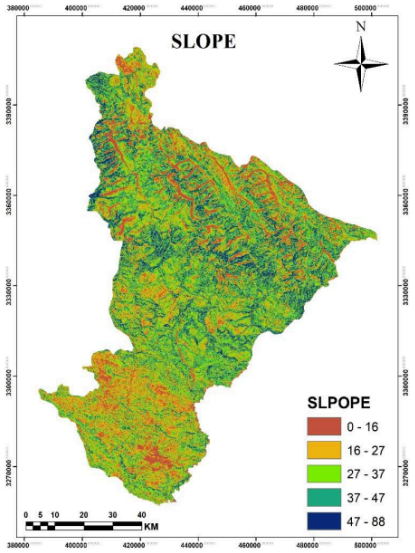

Fig. 4. Slope

3.3.2 Aspect

Aspect represents the direction of slope faces and influences moisture retention, vegetation cover, and weathering processes. Using the Spatial Analyst tools in ArcGIS, the aspect map was derived from the DEM and divided into nine directions: flat(-1-42), East(42-88), South-East(88-133), South(133-178), South-West(178-224), West(224-269), North-West(269-314), and North(314-359) to evaluate its effect on landslide occurrence. Among the different directions, the south and southwest-facing slopes showed the least susceptibility. The different level of susceptibility among the aspect classes is due to the fact that they retain varying amounts of moisture, have different levels of vegetation cover, and undergo weathering at different intensity as a result of varying exposure to the sun among the slope orientations in Pithoragarh.

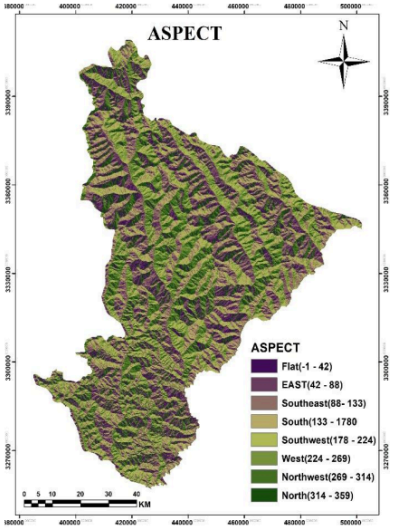

Fig. 5. Aspect

3.3.3 Hillshade

Aspect represents the direction of slope faces and influences moisture retention, vegetation on Hillshade, which reflects terrain illumination and surface orientation was derived from the DEM and the illumination parameter was reclassified into five levels representing increasing illumination conditions, from low to very high. These classes represent spatial variations in solar exposure, where low-illumination zones, typically associated with shadowed and moisture-retaining slopes, exhibit higher susceptibility to instability, while high-illumination areas generally correspond to well-exposed and relatively stable terrain. The hillshade classification provides valuable input for understanding terrain morphology and its influence on landslide occurrence.

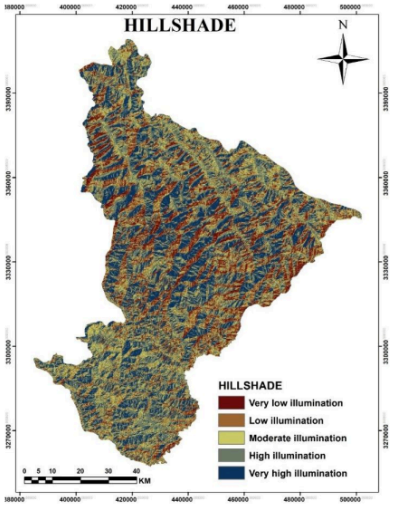

Fig. 6. Hillshade

3.3.4 Distance to Stream

The distance from a stream is a very significant factor in determining landslides because, among other things, stream flow causes toe erosion, slope undercutting, and increased soil saturation along valley sides. In the present study, a distance-from-stream layer was created via the Euclidean Distance tool in ArcGIS with its input being the stream network map within the study area. The produced raster was then divided into several distance classes for examining the spatial correlation between landslide occurrences and proximity to streams. Typically, locations adjacent to streams will manifest higher levels of landslide susceptibility because they are subject to constant erosion and high moisture conditions which result in decreased slope stability. On the other hand, areas further away from river channels are less inclined to be affected by the fluvial processes thus they generally reveal lower susceptibility. The use of the distance-from-stream variable makes it possible for the Frequency Ratio–based landslide susceptibility model to better show the hydrological controls.

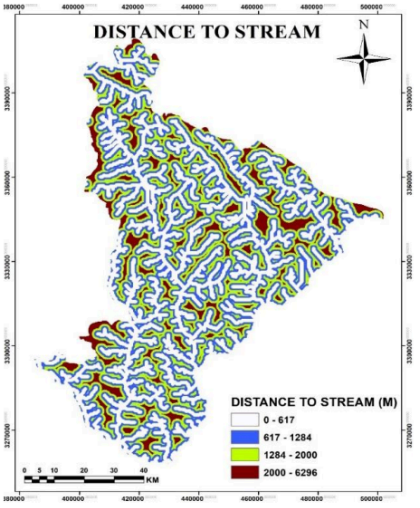

Fig. 7. Distance to stream

3.3.5 Lithology

The lithology layer of Pithoragarh District has been obtained from secondary geological data and was divided into four basic groups: unconsolidated sediments, soft sedimentary rocks, hard sedimentary rocks, and crystalline rocks. These rock types have different mechanical strength as well as weathering characteristics that indirectly affect slope stability and the location of landslides. The lithology map was created by extracting, rasterizing, and resampling at a 30 m resolution and then it was used in the Frequency Ratio–based landslide susceptibility study for analyzing the extent of the relationship between lithology and past land movements.

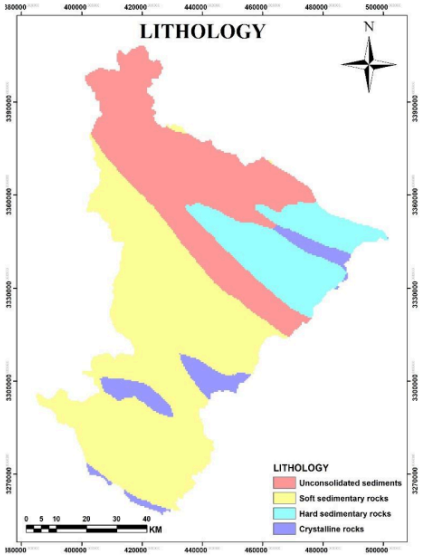

Fig. 8. Lithology

3.3.6 Curvature

Curvature is a quantitative representation of how quickly the slope changes, and it plays a significant role in landslide initiation because it influences the flow and concentration of surface water across the terrain. In order to obtain the curvature layer in this research, the Digital Elevation Model (DEM) was processed using the Spatial Analyst extension in ArcGIS. The produced curvature map was divided into three classes: highly concave, moderately concave, and flat to convex, for testing if landslides were influenced by these types of topography. The main reason why concave surfaces are more susceptible to landslides is that they generally support water sharing in the area as well as raise the pore water pressure, thus resulting in a higher degree of weakening of slopes. On the contrary, flattish to convex areas tend to provide natural drainage for runoff and are less prone to landslides. After that, the curvature layer was used as one of the explanatory variables in Frequency Ratio–based landslide susceptibility mapping.

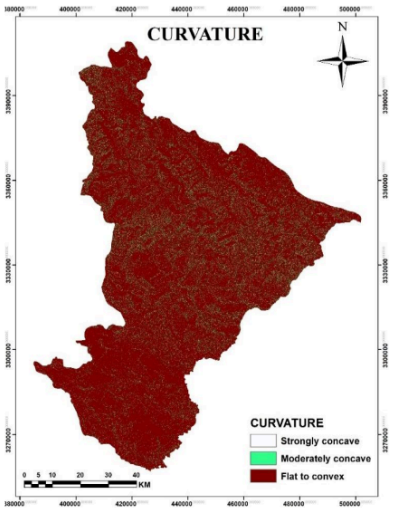

Fig. 9. Curvature

3.3.7 Distance to Road

A distance-to-road map was created to assess the spatial distribution of landslides relative to the closeness of roads. By utilizing the road network, a Euclidean distance operation was carried out in a GIS setting to produce the distance raster. The obtained map was divided into three distance categories: 0–2508 m, 2508–6484 m, and 6484–15600 m. This breakdown is useful in grasping how the frequency of landslide events changes with the increasing distance from roads. The distance to road layer was employed as one of the factors in the landslide susceptibility analysis.

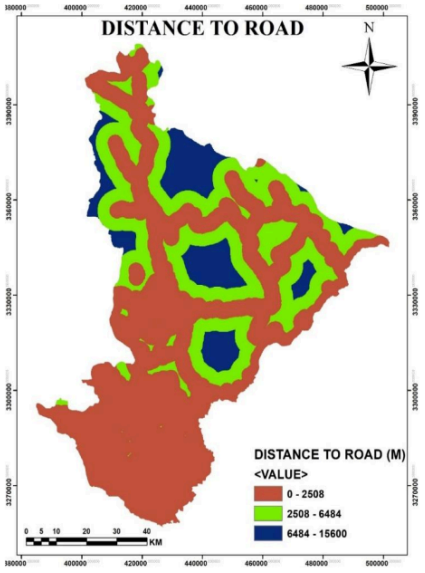

Fig. 10. Distance to road

3.3.8 Distance to Lineament

A distance to lineament map was created to show how the distance to geological lineaments varies spatially in the whole study area. Geological lineaments data were used to create a Euclidean distance raster layer in a GIS platform. The output distance values were divided into seven categories starting from 0-1441 m up to 11341-15979 m. This factor is a reflection of how much the distance from lineaments increases and was used as a separate variable in the landslide susceptibility assessment.

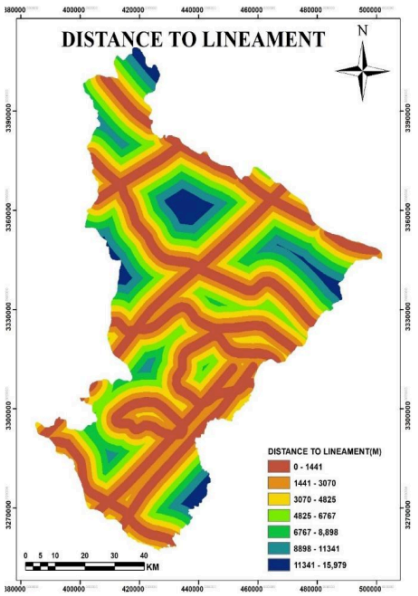

Fig. 11. Distance to lineament

3.3.9 Topographic Wetness Index (TWI)

The Topographic wetness index map was created using a DEM as a basis for deriving the topography variations that largely control soil moisture conditions in the study area. TWI values depict the water accumulation potential derived from slope and upstream contributing area. The generated TWI raster was divided into five categories (1–5, 5–7, 7–9, 9–14, and 14–33). Areas with high TWI values are those with maximum moisture concentration typically located at valley bottoms and drainage lines. On the other hand, low values indicate that ridge and slope regions are well-drained. This factor was applied to examine the effect of terrain-driven moisture on the second-level of landslide susceptibility.

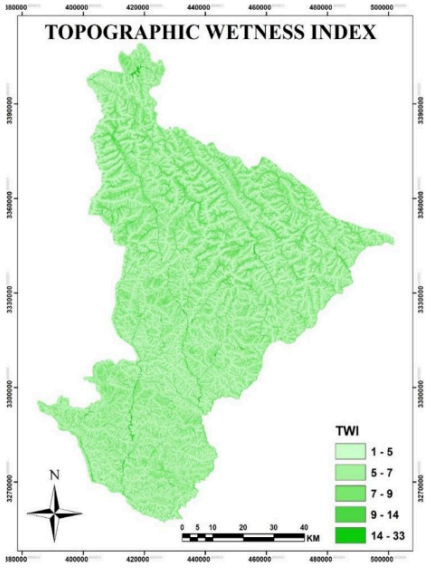

Fig. 12. TWI

3.3.10 Terrain Ruggedness Index

The Terrain Ruggedness Index (TRI) was extracted from the Digital Elevation Model (DEM) to represent surface roughness and elevation variability across the study area. TRI indicates the degree of terrain dissection and structural complexity, which significantly influences slope instability and landslide susceptibility. The generated TRI map was classified into five distinct categories: 0–28, 28–70, 70–126, 126–913, and 913–3583, each reflecting a specific level of topographic variation. Areas with lower TRI values are generally characterized by smooth, gently rolling landscapes, making them relatively stable and less vulnerable to mass movement. Conversely, regions exhibiting higher TRI values are predominantly steep, rugged, and heavily dissected, indicating greater structural complexity. Consequently, such areas demonstrate considerably higher susceptibility to landslide occurrence due to their pronounced surface roughness and topographic irregularity.

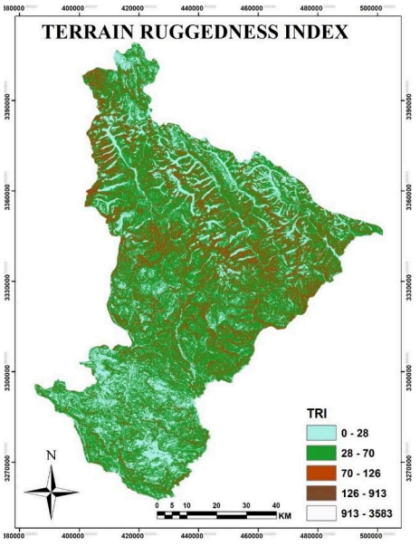

Fig. 13. TRI

3.4 FREQENCY RATIO MODEL

3.4.1 Introduction

A map layer was taken from the. The frequency Ratio (FR) method can be described as an empirical and data-driven approach that was first utilized to uncover the quantitative association between past landslide events and landslide conditioning factors (LCFs). It assesses the closeness of the spatial relationships between landslides and the separate classes of the factors in order to calculate their relative importance in slope de-stabilization.

3.4.2 Formula

- **Class Pixel**

Class Pixels (%) = (Pixels in Factor Class / Total Pixels in Study Area) × 100

This represents the percentage area occupied by each factor class.

$$\text{Class Pixels (\%)} = \left(\frac{P_C}{\sum_{i=1}^{n} P_C}\right) \times 100 \qquad \text{Eqs. (1)}$$

where P_C= Pixels of a factor class.

- **Landslide Pixel**

Landslide Pixels (%) = (Landslide Pixels in Class / Total Landslide Pixels) × 100

This represents the percentage distribution of landslides in each class.

$$\text{Landslide Pixels (\%)} = \left(\frac{P_L}{\sum_{i=1}^{n} P_L}\right) \times 100 \qquad \text{Eqs. (2)}$$

where P_L= Landslide pixels in a factor class.

- **Frequency Ratio**

FR = (Landslide Pixels in Factor Class / Total Landslide Pixels) ÷ (Total Pixels in Factor Class / Total Pixels in Study Area)

The resulting ratio represents the correlation strength between the factor class and landslide occurrence.

$$FR_i = \frac{\left(\frac{P_L}{\sum_{i=1}^{n} P_L}\right)}{\left(\frac{P_C}{\sum_{i=1}^{n} P_C}\right)} \quad \text{Eqs. (3)}$$

where P_L= Landslide pixels in a factor class,
P_C= Pixels of a factor class.

- **Total Frequency Fatio**

Total FR = Sum of all class-wise FR values

This is the total contribution of a conditioning factor to the outcome.

$$\sum FR = \sum_{i=1}^{n} F\,R_i \quad \text{Eqs. (4)}$$

- **Relative frequency (RF)**

RF = FR of a class / Total FR

This shows the differential weight of each class after normalization.

$$RF_i = \frac{FR_i}{\sum_{i=1}^{n} FR_i} \quad \text{Eqs. (5)}$$

RF (INT) = RF × 100

In GIS, we use this for raster reclassification.

$$RF_{INT} = RF_i \times 100 \quad \text{Eqs. (6)}$$

- **Min. and Max. RF and Range of RF (max. min.)**

Min RF = Minimum RF value of a factor Max RF = Maximum RF value of a factor
These are the boundary values for

$$RF_{min} = \min\,(RF_i), RF_{max} = \max\,(RF_i) \quad \text{Eqs. (7)}$$

Range = Max. RFi, Min. RFi
Here, we measure how factor influence has changed.

$$\Delta RF = RF_{max} - RF_{min} \quad \text{Eqs. (8)}$$

- **Normalized (RF) and Prediction rate (PR)**

Normalized RF = (RF, Min RF) / (Max RF, Min RF)

Values between 0 and 1 are standardized by this method.

$$RF_{norm} = \frac{RF_i - RF_{min}}{RF_{max} - RF_{min}} \quad \text{Eqs. (9)}$$

Prediction rate PR = (Max RF, Min RF) / Minimum standardized value

It sums up in how far each factor is really important.

$$PR = \frac{RF_{max} - RF_{min}}{RF^*_{min}} \quad \text{Eqs. (10)}$$

where RF^*_{min}= Minimum normalized value (taken as 0.050 in this study).

3.4.3 Implementation

It was a whole set of landslide conditioning factor (like slope, aspect, lithology, curvature, distance to streams etc), that were all classified significant classes. For every class, FR values were figured out, and consequently, the weights were given to those classes on the basis of their role in landslide occurrence. In other words, weighted thematic layers have been combined to produce the landslide susceptibility map.

3.4.4 Outcome

Using the FR methodology, weights are assigned to the raster representation of each conditioning factor. The aggregation of these weighted layers results in a landslide susceptibility map that highlights areas ranging from low to high susceptibility.

3.4.5 Advantages

One of the key advantages of the Frequency Ratio method is its simplicity and efficiency in analyzing landslide susceptibility. Since it is based on historical data, it provides objective and quantifiable results without relying on subjective expert opinions. Additionally, it is easy to implement using GIS software, making it a preferred choice for regional-scale susceptibility assessments.

Another significant advantage is its flexibility, which can be applied to various terrains and

environmental conditions. The method also allows for comparative analysis with other models, helping researchers and planners evaluate the effectiveness of different susceptibility assessment techniques. Furthermore, the statistical nature of FR improves accuracy, ensuring reliable hazard predictions in landslide-prone regions.

3.5.6 Application

FR is commonly applied in geospatial analysis using GIS tools to generate landslide susceptibility maps. The method enables accurate zoning of landslide- prone areas by integrating historical landslide data with environmental and topographical parameters. These susceptibility maps assist in disaster preparedness, infrastructure planning, and risk assessment, helping policymakers make informed decisions for mitigation strategies.

TABLE 2. FREQUENCY RATIO CALCULATION

Parameter	Classes	Class pixels	Class Pixels (%)	Landslide pixel	Landslide pixels (%)	FR	RF	RF (non%)	RF (INT)	Min RF	Max RF	(Max-Min) RF	(Max-Min) Min RF	PR
SLOPE (DEGREE)														
0 - 16	1	1285064	15.824	2016	6.568	0.415	0.069	6.927	6					
16- 27	2	2008852	24.736	4879	15.896	0.643	0.107	10.724	10					
27-37	3	2227427	27.427	5369	17.492	0.638	0.106	10.643	10					
37-47	4	1758546	21.654	9139	29.775	1.375	0.229	22.946	22					
26 47-88	5	841308	10.359	9291	30.270	2.922	0.488	48.761	48					
TOTAL		**8121196**		**30694**		**5.992**				**0.069**	**0.488**	**0.419**	**0.050**	**8.382**
ASPECT (DEGREE)														
Flat (-1-42)	1	946111	11.650	3228	10.517	0.903	0.112	11.167	11					

East (42-88)	2	975044	12.006	3282	10.693	0.891	0.110	11.017	11					
Southeast (88-133)	3	1076351	13.254	3499	11.400	0.860	0.106	10.640	10					
South (133-1780)	4	1132313	13.943	3606	11.748	0.843	0.104	10.424	10					
Southwest (178-224)	5	1112854	13.703	3614	11.774	0.859	0.106	10.630	10					
West (224-269)	6	1010533	12.443	4020	13.097	1.053	0.130	13.021	13					
Northwest (269-314)	7	883979	10.885	4473	14.573	1.339	0.166	16.562	16					
North (314-359)	8	984011	12.117	4972	16.199	1.337	0.165	16.538	16					
TOTAL		**8121196**		**30694**		**8.084**				**0.104**	**0.166**	**0.061**	**0.050**	**1.228**
HILLSHADE														
Very low illumination	1	984142	12.128	3146	10.264	0.846	0.170	17.043	17					
Low illumination	2	1348735	16.621	5576	18.192	1.095	0.220	22.042	22					
Moderate illumination	3	1743483	21.486	7170	23.393	1.089	0.219	21.926	21					
High illumination	4	1996130	24.599	7637	24.917	1.013	0.204	20.398	20					
Very high illumination	5	2042177	25.166	7121	23.233	0.923	0.186	18.591	18					
TOTAL		**8114667**		**30650**		**4.966**				**0.170**	**0.220**	**0.050**	**0.050**	**1**
DISTANCE TO STREAM (METERS)														
0-617	1	3072358	37.754	17375	56.475	1.496	0.437	43.714	43					
617-1284	2	2494524	30.653	7501	24.381	0.795	0.232	23.243	23					
1284-2000	3	1831591	22.507	4577	14.877	0.661	0.193	19.316	19					
2000-6296	4	739407	9.086	1313	4.268	0.470	0.137	13.726	13					

TOTAL		**8137880**		**30766**		**3.422**				**0.137**	**0.437**	**0.300**	**0.050**	**5.999**
LITHOLOGY														
Unconsolidated sediments	1	2044728	25.175	600	1.978	0.079	0.024	2.387	2					
Soft sedimentary rocks	2	1519000	18.702	4023	13.260	0.709	0.215	21.549	21					
Hard sedimentary rocks	3	2984477	36.745	23278	76.726	2.088	0.635	63.460	63					
Crystalline rocks	4	1573862	19.378	2438	8.036	0.415	0.126	12.604	12					
TOTAL		**8122067**		**30339**		**3.290**				**0.024**	**0.635**	**0.611**	**0.050**	**12.218**
CURVATURE														
Strongly concave	1	1248273	15.339	4330	14.063	0.917	0.330	32.999	32					
Moderately concave	2	5719995	70.288	22906	74.394	1.058	0.381	38.096	38					
Flat to convex	3	1169723	14.347	3554	11.543	0.803	0.289	28.904	28					
TOTAL		**8137991**		**30790**		**2.778**				**0.289**	**0.381**	**0.092**	**0.050**	**1.839**
DISTANCE TO ROAD (METERS)														
0-2508	1	4233393	52.021	30376	98.732	1.898	0.974	97.363	97					
2508-6484	2	2077787	25.532	290	0.943	0.037	0.019	1.894	1					
6484-15600	3	1826700	22.447	100	0.325	0.014	0.007	0.743	0					
TOTAL		**8137880**		**30766**		**1.949**				**0.007**	**0.974**	**0.966**	**0.050**	**19.329**
DISTANCE TO LINEAMENT (METERS)														
0-1441	1	2075842	25.508	9306	30.248	1.186	0.184	18.393	18					

1441- 3070	2	1775721	21.820	8136	26.445	1.212	0.188	18.798	18					
3070-4825	3	1387731	17.053	5369	17.451	1.023	0.159	15.873	15					
4825-6767	4	1129941	13.885	2966	9.641	0.694	0.108	10.769	10					
6767-8998	5	861690	10.589	2228	7.242	0.684	0.106	10.608	10					
8898-11341	6	595538	7.318	1721	5.594	0.764	0.119	11.856	11					
11341-15979	7	311417	3.827	1040	3.380	0.883	0.137	13.702	13					
TOTAL		**8137880**		**30766**		**6.447**				**0.106**	**0.188**	**0.082**	**0.050**	**1.638**
TOPOGRAPHIC WETNESS INDEX (TWI)														
1-5	1	2731797	33.569	9626	31.293	0.932	0.142	14.211	14					
5-7	2	3318948	40.784	12664	41.169	1.009	0.154	15.389	15					
7-9	3	1543886	18.972	5717	18.585	0.980	0.149	14.934	14					
9-14	4	439776	5.404	1741	5.660	1.047	0.160	15.966	15					
14-33	5	103430	1.271	1013	3.293	2.591	0.395	39.500	39					
TOTAL		**8137837**		**30761**		**6.560**				**0.142**	**0.395**	**0.253**	**0.050**	**5.059**
TERRAIN RUGGEDNESS INDEX (TRI)														
0-28	1	2879366	35.569	12285	40.122	1.131	0.314	31.398	31					
28- 70	2	3179497	39.184	12752	41.647	1.063	0.295	29.515	29					
70-126	3	1667168	20.546	4589	14.987	0.729	0.203	20.257	20					
126-913	4	388089	4.783	993	3.243	0.678	0.188	18.830	18					
913-3583	5	152	0.002	0	0	0	0	0	0					

TOTAL		8114272		30619		3.601				0.188	0.314	0.126	0.050	2.514

3.5 Shannon Entropy Model

3.5.1 Introduction

The Entropy is a key notion in information theory that measures the degree of unpredictability or disorder in a system. It measures how much information is needed to specify a random variable and is a fundamental concept in characterizing the uncertainty of a system. In the field of spatial analysis and landslide susceptibility mapping (LSM), The Shannon Entropy model is applied to estimate the weight and relative importance of selected conditioning factors that influence landslide susceptibility, including slope, lithology, distance to streams, and distance to roads etc. Calculating the entropy of these variables allows one to determine the extent to which each variable contributes to the spatial pattern of landslides, thus facilitating accurate and dependable identification of areas prone to landslides. This method helps in lessening uncertainty and expanding the knowledge of landslide risk.

3.5.2 Formula

$$\%FR = \frac{\%\ Landslide\ pixels}{\%\ Class\ pixels} \qquad \text{Eqs. (11)}$$

Where P_{ij} from equation 11 represents frequency ratio and (P_{ij}) from equation 12 gives probability density value of each class

$$(P_{ij}) = \frac{(P_{ij})}{\sum_1^n P_{ij}} \qquad \text{Eqs. (12)}$$

E_{ij} and E_{ijmax} from equation 13 and 14 denote the entropy values for each class whereas n_{ij} is the number of classes in each factor

$$E_{ij} = \sum_{i=1}^{n_j}(P_{ij}) \times log(P_{ij}) \qquad \text{Eqs. (13)}$$

$$E_{ijmax} = \log_2(n_{ij}) \quad \text{Eqs. (14)}$$

The information coefficient, I_j, and the final weight index, W_j were evaluated using equations 15 and 16 respectively

$$I_{ij} = \frac{H_{jmax} - H_j}{H_{jmax}} \quad \text{Eqs. (15)}$$

$$W_j = I_j \times P_j \quad \text{Eqs. (16)}$$

3.5.3 Implementation

Firstly, the FR of each factor of Slope, Lithology, TWI, etc. should be calculated as a step towards implementing the Shannon Entropy model in ArcGIS. This can be done by overlaying the landslide points and the factor classes. The Field Calculator is the tool you would use to compute the probability density (Pij), entropy (Ej), and the final weights (Wj) in your attribute table. At last, assign (FR) values to the respective rasters through the Reclassify method and sum up the weighted factors (Wj×FR) by using Raster Calculator for your final susceptibility map.

3.5.4 Outcome

The result of applying Shannon Entropy for landslide susceptibility mapping refers to the production of normalized entropy values that function as weights to determine the contribution of each landscape classification factor (LCF) to landslide susceptibility. The normalized entropy values reveal the level or intensity of contribution of each factor, e.g. slope, aspect, or curvature to the probability of landslides in the area. Together with these weights, the different LCFs are used to produce an improved and more precise landslide susceptibility map. This map delineates risk zones of landslides at various scales and thus provides a very useful geographically relevant risk assessment tool to help in risk management and mitigation strategies.

3.5.5 Advantages

It has a lot of benefits when it is applied in landslide susceptibility mapping (LSM). It introduces an unbiased and based-on-data technique for measuring the impact of each landslide

condition factor, thus lessening the human element in assigning weights. The approach successfully copes with the unknowns and changeability in spatial data, which makes it a good match for complicated areas like the Pithoragarh district. Besides, it is compatible with GIS software, which enables quick spatial analyses and the production of maps. On top of that, Shannon Entropy is not dependent on large quantities of verification data on the ground because it makes use of the statistical interactions between landslide events and environmental factors. By producing normalized weights it contributes to the generation of more precise and trustworthy susceptibility maps, which are instrumental in effective risk assessment and incident management.

3.5.6 Application

A landslide inventory is primarily a record of landslides that have occurred through the time, while the conditioning factors are the environmental and topographical variables that mainly influence the potential for landslide occurrence. Based on these elements, Shannon Entropy quantifies the level of uncertainty and the comparative importance of each factor contributing to landslide susceptibility with in a particular study area.

TABLE 3. SHANNON ENTROPY CALCULATION

Parameter	Classes	Class pixels	Class Pixels (%)	Landslide pixel	Landslide pixels (%)	FR	Shannon Entropy			
							Pij	Eij	1-Eij	Wj
SLOPE (DEGREE)										
0 - 16	1	1285064	15.824	2016	6.568	0.415	0.069	-0.080		
16- 27	2	2008852	24.736	4879	15.896	0.643	0.107	-0.104		
27-37	3	2227427	27.427	5369	17.492	0.638	0.106	-0.104		
37-47	4	1758546	21.654	9139	29.775	1.375	0.229	-0.147		
26 47-88	5	841308	10.359	9291	30.270	2.922	0.488	-0.152		

TOTAL		**8121196**		**30694**		**5.992**	**1**	**0.974**	**0.026**	**0.014**
ASPECT (DEGREE)										
Flat (-1-42)	1	946111	11.650	3228	10.517	0.903	0.112	-0.106		
East (42-88)	2	975044	12.006	3282	10.693	0.891	0.110	-0.106		
Southeast (88-133)	3	1076351	13.254	3499	11.400	0.860	0.106	-0.104		
South (133-1780)	4	1132313	13.943	3606	11.748	0.843	0.104	-0.102		
Southwest (178-224)	5	1112854	13.703	3614	11.774	0.859	0.106	-0.103		
West (224-269)	6	1010533	12.443	4020	13.097	1.053	0.130	-0.115		
Northwest (269-314)	7	883979	10.885	4473	14.573	1.339	0.166	-0.129		
North (314-359)	8	984011	12.117	4972	16.199	1.337	0.165	-0.129		
TOTAL		**8121196**		**30694**		**8.084**	**1**	**0.991**	**0.009**	**0.005**
HILLSHADE										
Very low illumination	1	984142	12.128	3146	10.264	0.846	0.170	-0.131		
Low illumination	2	1348735	16.621	5576	18.192	1.095	0.220	-0.145		
Moderate illumination	3	1743483	21.486	7170	23.393	1.089	0.219	0.145		
High illumination	4	1996130	24.599	7637	24.917	1.013	0.204	-0.141		
Very high illumination	5	2042177	25.166	7121	23.233	0.923	0.186	-0.136		
TOTAL		**8114667**		**30650**		**4.966**	**1**	**0.997**	**0.003**	**0.002**
DISTANCE TO STREAM (METERS)										
0-617	1	3072358	37.754	17375	56.475	1.496	0.437	-0.157		

617-1284	2	2494524	30.653	7501	24.381	0.795	0.232	-0.147		
1284-2000	3	1831591	22.507	4577	14.877	0.661	0.193	-0.138		
2000-6296	4	739407	9.086	1313	4.268	0.470	0.137	-0.118		
TOTAL		**8137880**		**30766**		**3.422**	**1**	**0.931**	**0.069**	**0.038**
LITHOLOGY										
Unconsolidated sediments	1	2044728	25.175	600	1.978	0.079	0.026	-0.041		
Soft sedimentary rocks	2	1519000	18.702	4023	13.260	0.709	0.234	-0.148		
Hard sedimentary rocks	3	2984477	36.745	23278	76.726	2.088	0.690	-0.111		
Crystalline rocks	4	1573862	19.378	2438	8.036	0.415	0.050	-0.065		
TOTAL		**8122067**		**30339**		**3.290**	**1**	**0.607**	**0.393**	**0.217**
CURVATURE										
Strongly concave	1	1248273	15.339	4330	14.063	0.917	0.330	-0.159		
Moderately concave	2	5719995	70.288	22906	74.394	1.058	0.381	-0.160		
Flat to convex	3	1169723	14.347	3554	11.543	0.803	0.289	-0.156		
TOTAL		**8137991**		**30790**		**2.778**	**1**	**0.788**	**0.212**	**0.117**
DISTANCE TO ROAD (METERS)										
0-2508	1	4233393	52.021	30376	98.732	1.898	0.974	-0.011		
2508-6484	2	2077787	25.532	290	0.943	0.037	0.019	-0.033		
6484-15600	3	1826700	22.447	100	0.325	0.014	0.007	-0.016		
TOTAL		**8137880**		**30766**		**1.949**	**1**	**0.125**	**0.875**	**0.482**

DISTANCE TO LINEAMENT (METERS)										
0-1441	1	2075842	25.508	9306	30.248	1.186	0.184	-0.135		
1441- 3070	2	1775721	21.820	8136	26.445	1.212	0.188	-0.136		
3070-4825	3	1387731	17.053	5369	17.451	1.023	0.159	-0.127		
4825-6767	4	1129941	13.885	2966	9.641	0.694	0.108	-0.104		
6767-8998	5	861690	10.589	2228	7.242	0.684	0.106	-0.103		
8898-11341	6	595538	7.318	1721	5.594	0.764	0.119	-0.110		
11341-15979	7	311417	3.827	1040	3.380	0.883	0.137	-0.118		
TOTAL		**8137880**		**30766**		**6.447**	**1**	**0.987**	**0.013**	**0.007**
TOPOGRAPHIC WETNESS INDEX (TWI)										
1-5	1	2731797	33.569	9626	31.293	0.932	0.142	-0.120		
5-7	2	3318948	40.784	12664	41.169	1.009	0.154	-0.125		
7-9	3	1543886	18.972	5717	18.585	0.980	0.149	-0.123		
9-14	4	439776	5.404	1741	5.660	1.047	0.160	-0.127		
14-33	5	103430	1.271	1013	3.293	2.591	0.395	-0.159		
TOTAL		**8137837**		**30761**		**6.560**	**1**	**0.938**	**0.062**	**0.034**
TERRAIN RUGGEDNESS INDEX (TRI)										
0-28	1	2879366	35.569	12285	40.122	1.131	0.314	-0.158		
28- 70	2	3179497	39.184	12752	41.647	1.063	0.295	-0.156		

70-126	3	1667168	20.546	4589	14.987	0.729	0.203	-0.140		
126-913	4	388089	4.783	993	3.243	0.678	0.188	-0.137		
913-3583	5	152	0.002	0	0	0	0	0		
TOTAL		**8114272**		**30619**		**3.601**	**1**	**0.846**	**0.154**	**0.085**

3.6 Analytical Hierarchy Process

3.6.1 Introduction

The Analytical Hierarchy Process (AHP), introduced by Saaty (1980), is a multi-criteria decision-making method that derives factor weights from structured expert judgment through pairwise comparisons. The AHP method differs from the FR and SE approaches by employing expert-based pairwise comparisons to determine the relative influence of Landslide Conditioning Factors. This hierarchical procedure ensures that expert knowledge is incorporated in a logical and consistent way.

3.6.2 Formula

A 10×10 pairwise comparison matrix was constructed for the ten conditioning factors — Distance to Road, Lithology, Slope, Distance to Stream, TWI, TRI, Curvature, Distance to Lineament, Aspect, and Hillshade — using Saaty's 1–9 scale. The priority weight vector W was derived by solving the principal eigenvector equation:

$$AW = \lambda\_max \times W \qquad \text{Eqs. (17)}$$

where **A** is the pairwise comparison matrix, W is the normalized weight vector, and λ_max is the principal eigenvalue. The internal consistency of the expert judgments was evaluated using the CI and CR:

$$CI = (\lambda\_max - n) / (n - 1) \qquad \text{Eqs. (18)}$$

$$CR = (CI / RI) \qquad \text{Eqs. (19)}$$

where n = 10 is the number of factors and RI = 1.49 is the Random Index for a 10×10 matrix. The computed values were λ_max = 10.111, CI = 0.012, and CR = 0.008. As the CR value was well below 0.10, the judgments provided by the experts were deemed reliable and internally consistent.

3.6.3 Implementation

The pairwise comparison matrix was populated using expert judgment, with each factor rated relative to all others according to its influence on slope instability in the Pithoragarh context. The normalized eigenvector method was applied to extract the final priority weights (Wj), which ranged from 0.02 for Hillshade to 0.20 for Distance to Road. The three most influential factors identified through AHP were Distance to Road (Wj = 0.20), Lithology (Wj = 0.18), and Slope (Wj = 0.14), consistent with the factor rankings produced by the FR and SE models.

In ArcGIS 10.8, each conditioning factor raster was reclassified using the Reclassify tool to assign normalized class ratings (NRj). The Landslide Susceptibility Index was then computed using the Raster Calculator as a weighted linear combination:

$$LSM = \Sigma (Wj \times NRj), \text{ for } j = 1 \text{ to } 10 \qquad \text{Eqs. (20)}$$

3.6.4 Outcome

The susceptibility assessment based on AHP resulted in five zonation classes, with 20.1%, 18.4%, 9.2%, 23.0%, and 29.2% of the area falling under the Very Low, Low, Moderate, High, and Very High categories. The combined High and Very High zones covered 52.2% of the district, closely matching the SE model's 52.1% and exceeding the FR model's 42.3%, indicating that expert-based and entropy-based weighting approaches converge in overall hazard delineation despite their fundamentally different methodological bases. Field validation confirmed that 95.9% of the 366 documented landslide inventory points fell within the combined High and Very High susceptibility zones. On the independent 30% testing dataset, the AHP model achieved the highest prediction accuracy among the three models with an AUC of 0.839 on the Prediction Rate Curve, placing it in the "very good" performance category. The Consistency Ratio of 0.008 — well below the 0.10 benchmark

— confirmed the internal logical coherence of the expert pairwise judgments underpinning the AHP weighting framework.

3.4.5 Advantages

Firstly, it introduces a structured framework for the inclusion of expert judgment and their involvement in the evaluation of landslide conditioning factors, thereby, making it a systematic evaluation. Second, during the implementation, it carries out pairwise comparisons, ensures the derived weights are reliable by validating through Consistency Ratio and maintains consistency. This technique can easily and flexibly be incorporated with GIS tools like ArcGIS. Lastly, the results presented from the AHP are scientifically weighted Landslide Susceptibility Maps that at once are able to expose high-risk locations and serve as a ground for the informed decision-making with the aim of hazard mitigation, land-use planning, and sustainable development in regions affected by landslide activity.

3.5.6 Application

The Analytical Hierarchy Process serves as a structured framework for evaluating and prioritizing alternatives in multi-criteria decision-making scenarios. In the field of landslide studies, it is applied to create susceptibility maps by assigning weights to conditioning factors such as slope, lithology, and drainage based on their relative influence on slope failure.

Beyond geotechnical applications, AHP is also used in urban planning, site selection, resource allocation, environmental impact assessment, and risk analysis. It supports decision-makers in evaluating alternatives where both qualitative (expert opinion) and quantitative data are involved.

A 10 × 10 pairwise comparison matrix was prepared using expert knowledge, where the relative importance of each factor was determined through Saaty's 1–9 rating system. Priority weights were computed through the normalized eigenvector method. The Consistency Ratio (CR) was calculated as 0.008, well below the acceptable threshold of 0.10, confirming that the expert judgments were logically consistent and free of significant contradictions.

It is commonly referred to as the 'AHP fundamental scale of Preference' or the saaty's Nine Point Importance scale, "introduced by Thomas L. Saaty (1980) which is shown in table 4.

TABLE 4. SAATY'S PAIRWISE COMPARISON SCALE RATING

Numerical Value	Preference Level	Interpretation
1	Equal importance	The two factors contribute equally; neither is favored over the other.
3	Slight preference	One factor is marginally more important based on experience or judgment.
5	Considerable preference	One factor holds a clear and demonstrable advantage over the other.
7	Strong dominance	One factor is substantially more influential; this superiority is practically evident.
9	Absolute dominance	One factor outweighs the other to the maximum extent that can be reasonably justified.
2, 4, 6, 8	Transitional values	Applied when a judgment falls between two consecutive preference levels and a compromise is warranted.
Reciprocal (1/x)	Reverse comparison	When factor B is assigned value x over factor A, then factor A automatically receives 1/x over factor B.

TABLE 5. AHP PAIRWISE COMPARISON MATRIX

	DISTANCE TO ROAD	LITHOLOGY	SLOPE	DISTANCE TO STREAM	TWI	TRI	CURVATURE	DISTANCE TO LINEAMENT	ASPECT	HILLSHADE
DISTANCE TO ROAD	**1**	1	2	2	2	3	3	3	5	9
LITHOLOGY	**1**	1	1	2	2	2	3	3	4	8
SLOPE	0.50	1	1	1	2	2	2	2	3	7
DISTANCE TO STREAM	0.50	0.50	1	1	1	2	2	2	3	6
TWI	0.50	0.50	0.50	1	1	1	2	2	3	5
TRI	0.33	0.50	0.50	0.50	1	1	1	1	2	4
CURVATURE	0.33	0.30	0.50	0.50	0.50	1	1	1	2	3
DISTANCE TO LINEAMENT	0.33	0.30	0.50	0.50	0.50	1	1	1	2	3
ASPECT	0.20	0.25	0.33	0.33	0.33	0.50	0.50	0.50	1	2
HILLSHADE	0.11	0.125	0.142	0.166	0.50	0.25	0.33	0.33	0.50	1
TOTAL	4.81	5.54	7.48	9	10.53	13.75	15.83	15.83	25.50	48

TABLE 6. CI AND CR

FACTOR	DSITANCE TO ROAD	LITHOLOGY	SLOPE	DISTANCE TO STREAM	TWI	TRI	CURVATURE	DISTANCE TO LINEAMENT	ASPECT	HILLSHADE	AVG.	λmax	CI	RCI	CR
DSITANCE TO ROAD	0.21	0.18	0.27	0.22	0.19	0.22	0.19	0.19	0.20	0.19	0.20	10.20			
LITHOLOGY	0.21	0.18	0.13	0.22	0.19	0.15	0.19	0.19	0.16	0.17	0.18	10.19			
SLOPE	0.10	0.18	0.13	0.11	0.19	0.15	0.13	0.13	0.12	0.15	0.14	10.19			
DISTANCE TO STREAM	0.10	0.09	0.13	0.11	0.09	0.15	0.13	0.13	0.12	0.13	0.12	10.18			
TWI	0.10	0.09	0.07	0.11	0.09	0.07	0.13	0.13	0.12	0.10	0.10	10.18			
TRI	0.07	0.09	0.07	0.06	0.09	0.07	0.06	0.06	0.08	0.08	0.07	10.18	0.012	1.49	0.008
CURVATURE	0.07	0.06	0.07	0.06	0.05	0.07	0.06	0.06	0.08	0.06	0.06	10.17			
DISTANCE TO LINEAMENT	0.07	0.06	0.07	0.06	0.05	0.07	0.06	0.06	0.08	0.06	0.06	10.17			
ASPECT	0.07	0.05	0.04	0.04	0.03	0.04	0.03	0.03	0.04	0.04	0.04	9.48			
HILLSHADE	0.02	0.02	0.02	0.02	0.02	0.02	0.02	0.02	0.02	0.02	0.02	10.17			

TABLE 7. RCI VALUES

n	9	10	11	12	13	14	15
RI	1.45	1.49	1.51	1.48	1.56	1.57	1.58

CHAPTER 4

RESULTS AND DISCUSSION

The spatial distribution of landslide susceptibility was evaluated using FR, SE, and AHP approaches. AHP was adopted as one of the modelling techniques because it offers a systematic procedure for assigning relative importance to multiple conditioning factors based on pairwise comparisons and expert. These models identify landslide-prone areas by integrating conditioning factors such as slope, hillshade, aspect, and lithology within a GIS-based framework. Owing to differences in their computational principles each method produces varying susceptibility zonation.

4.1 Frequency Ratio (RF)

Model was employed to assess the spatial relationship between each landslide conditioning factor and historical landslide occurrences within the study area. The Predictive Ratio (PR) values derived from the FR analysis revealed that Distance to Road exhibited the highest influence on landslide susceptibility, recording a PR of 19.329, followed by Lithology (PR = 12.218) and Slope (PR = 8.382). These values indicate that proximity to road networks significantly disturbs slope stability through excavation and increased surface runoff, while lithological composition and slope gradient remain fundamental geomorphological drivers of mass movement in the Himalayan terrain. Distance to Stream (PR = 5.999) and Topographic Wetness Index (PR = 5.059) also demonstrated considerable influence, reflecting the role of hydrological conditions in triggering landslides. In contrast, parameters such as Hillshade (PR = 1.000), Aspect (PR = 1.228), and Distance to Lineament (PR = 1.638) exhibited comparatively lower predictive ratios, suggesting a relatively limited direct contribution to landslide occurrence in the study region.

4.2 The Shannon Entropy (SE)

Model was applied to quantify the information content and disorder associated with each conditioning factor, thereby determining their relative weights in landslide susceptibility

mapping. The computed entropy-based weights (Wj) confirmed that Distance to Road contributed the most significant weight (Wj = 0.482), underlining its dominant role as a destabilizing anthropogenic factor. Lithology followed with a Wj of 0.217, reinforcing the critical influence of geological composition on slope failure potential. Curvature (Wj = 0.117) and Terrain Ruggedness Index (Wj = 0.085) demonstrated moderate entropy-based importance, while Distance to Stream (Wj = 0.038) and TWI (Wj = 0.034) reflected a secondary hydrological influence. Factors such as Slope (Wj = 0.014), Distance to Lineament (Wj = 0.007), Aspect (Wj = 0.005), and Hillshade (Wj = 0.002) recorded the lowest entropy weights, indicating minimal informational variability with respect to landslide distribution. The broad agreement in factor rankings between the Shannon Entropy and Frequency Ratio models lends credibility to the identified conditioning hierarchy.

4.3 The Analytical Hierarchy Process (AHP)

It was utilized as a knowledge-driven, expert-based multi-criteria decision-making approach to systematically assign weights to the landslide conditioning factors through a structured pairwise comparison matrix, wherein each factor was evaluated against every other factor in terms of its relative importance to landslide susceptibility. This approach integrates domain expertise and professional judgment into the weighting process, providing a structured and transparent mechanism for incorporating qualitative assessments alongside quantitative data in the susceptibility mapping framework. The normalized priority weights derived from the AHP pairwise comparison matrix indicated that Distance to Road (weight ≈ 0.20) and Lithology (weight ≈ 0.18) were assigned the highest importance, a finding that is consistent with the results obtained from both the Frequency Ratio and Shannon Entropy models, thereby reinforcing the dominant role of anthropogenic disturbance and geological composition in governing slope instability within the study area. Slope (≈ 0.14) and Distance to Stream (≈ 0.12) followed as significant morphometric and hydrological contributors, acknowledging the well-established relationship between terrain gradient, fluvial proximity, and landslide triggering mechanisms in steep mountainous environments. TWI (≈ 0.10), TRI (≈ 0.07), Curvature (≈ 0.06), and Distance to Lineament (≈ 0.06) were accorded moderate weights, reflecting their recognized but comparatively secondary roles in influencing moisture distribution, surface roughness, slope geometry, and structural geological

discontinuities that may predispose terrain to failure. Aspect (≈ 0.04) and Hillshade (≈ 0.02) received the lowest priority weights in the AHP framework, reflecting their comparatively subordinate role in directly conditioning landslide susceptibility, though their indirect influence through differential weathering and solar radiation exposure was duly acknowledged. Critically, the Consistency Ratio (CR ≈ 0.008) of the pairwise comparison matrix remained below the widely accepted threshold of 0.10, confirming the logical coherence, internal consistency, and reliability of the expert judgments incorporated into the AHP framework, and thereby validating the integrity of the weight assignment process. The broad convergence in factor importance rankings observed across all three models — the FR, SE and AHP — collectively strengthens confidence in the robustness and validity of the landslide susceptibility assessment, suggesting that despite their fundamentally different methodological underpinnings, all three approaches consistently identify the same set of dominant conditioning factors Thus, the results can serve as a dependable scientific foundation for landslide hazard mitigation and informed land-use planning within the study area.

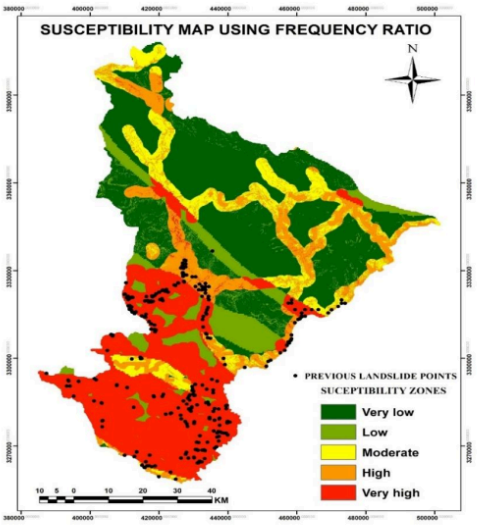

Fig. 14. LSM by FR model

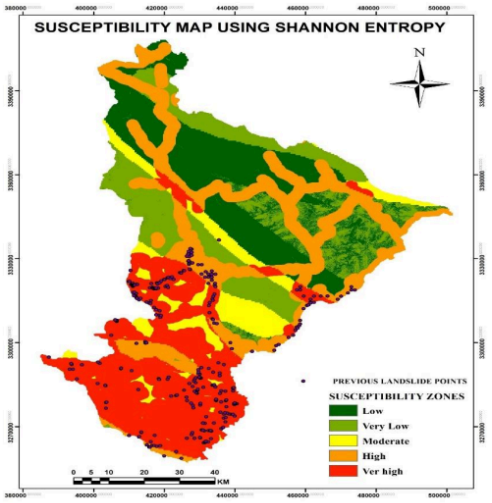

Fig. 15. LSM by SE model

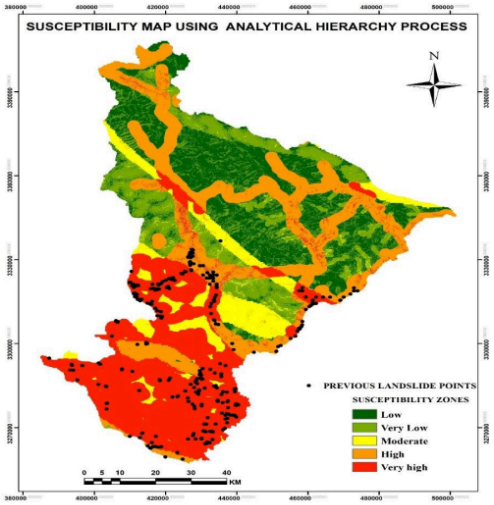

Fig. 16. LSM by AHP model

4.2 Validation

4.2.1 Model Validation Using Success Rate Curves

All three methods reliably and scientifically identify the major landslide influencing factors yet providing a strong basis for risk management of landsliding and land use planning in the study area. The ability to predict of all the three models was checked one more time by the construction of success rate curves. These curves resulted from the plotting of the cumulative appearance percentages of landslides against the respective susceptibility ranking that were derived from 70% of the landslide inventory which was used as the training dataset. The Area Under the Curve (AUC) values that were obtained from the success rate curves indicated that the AHP model showed the best result with an AUC of 0.830. It was closely followed by the Shannon Entropy model which had an AUC of 0.826, whereas the FR model had an AUC of 0.819. The three models have a very good to strong expenditure on the prediction as their AUC values are well above 0.5 which is a random guess. They have therefore confirmed reliability in detecting the spatial patterns of landslide susceptibility in the study area. The slight difference in AUC values among the three models indicate that their performance is approximately equal. AHP is marginally better mainly because it entails a systematic expert-based pairwise weighting of the conditioning factors.

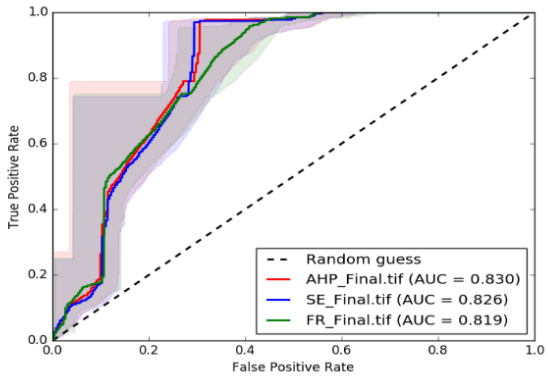

Fig. 17. SRC

These three models have very good to strong capability in predicting as their AUC values are way above the 0.5 level which is a random guess. Together, these results support that blending both knowledge-driven and data-driven methods produces a reliable and potent framework for assessing the landslide susceptibility in the rugged physiographic conditions of the study region. One crucial measure of validation is the success rate curve, which assess how well the model predicts the landslide-prone areas based on the training dataset. It is generated by plotting the cumulative percentage of correctly predicted landslide areas against the total study area. A higher success rate indicates that the model effectively captures patterns in the training data and is well-calibrated for mapping susceptibility.

4.2.3 Model Validation Using Prediction Rate Curves

On the other hand, the generalization capability and predictive accuracy of all three landslide susceptibility models were additionally assessed by means of prediction rate curves. The curves were generated by mapping the cumulative proportion of observed landslides against the respective susceptibility ranks assigned by the models. The ranks were taken from the 30% of the landslide inventory that had been set aside solely as the validation dataset. This way, the prediction rate curves served as an independent and unbiased evaluation of each model's capacity to forecast future or unknown landslide incidents.

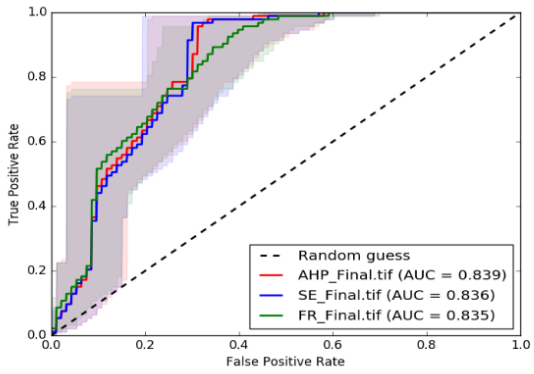

Fig. 18. PRC

The prediction rate curves showed that AHP model had the highest AUC of 0.839, Shannon Entropy was a very close second with 0.836, and Frequency Ratio followed with 0.835. Properly interpreting Swets (1988), AUC values between 0.80 and 0.90 fall within the "very good" performance category, confirming that all three models demonstrated strong and dependable predictive capability. The narrow AUC range of just 0.004 across all three models further indicates broadly comparable and consistent predictive performance, collectively affirming the robustness of the susceptibility framework applied in this study.

The slight yet still steady uplift in AUC values from the success rate to the prediction rate curves for the three models is a sure sign that there is no overfitting and it also shows that the models have strong generalization ability on independent validation data. The AHP model retained a slight advantage across both validation measures, attributable to its structured expert-based weighting framework, while the SE and FR models performed competitively, validating the reliability of data-driven statistical approaches for landslide susceptibility assessment in this geologically complex Himalayan environment.

The AUC scores attained in this study are at or above the range typically reported by comparable landslide susceptibility studies conducted in similar geological and climatic settings, confirming that the methodology employed here is not only internally consistent but also externally competitive. The close agreement in both validation metrics and conditioning factor rankings across all three models collectively affirms the scientific credibility of the susceptibility maps generated for Pithoragarh District, providing a dependable spatial basis for landslide hazard evaluation, disaster risk reduction, and infrastructure planning in the region.

CHAPTER 5

CONCLUSION

This study assessed landslide susceptibility across the 7217.7 km² of Pithoragarh District, Uttarakhand, using three methodologically distinct approaches —FR, SE and AHP applied to a comprehensive inventory of 366 historical landslide events and ten conditioning factors. These factors, encompassing both natural variables such as slope, lithology, curvature, TWI, TRI, aspect, hillshade, and distance to stream and lineament, and the anthropogenic variable of distance to road, provided a thorough spatial framework for evaluating the drivers of slope instability in this complex Himalayan terrain.

Distance to Road and Lithology were consistently identified as the two most dominant conditioning factors across all three models, underscoring the critical destabilizing role of road construction through fragile hillslopes and the inherent susceptibility of hard sedimentary rock units prevalent in the region. Slope and Distance to Stream emerged as significant secondary contributors, reflecting the combined influence of topographic gradient and hydrological conditions on landslide triggering. Field validation confirmed that more than 93.7% of all 366 inventory landslide points fell within the combined High and Very High susceptibility zones across all three models, with the SE and AHP models each capturing over 95% of recorded events.

Model performance evaluated through SRC and PRC demonstrated that all three models achieved very good predictive accuracy, with prediction rate AUC values of 0.835, 0.836, and 0.839 for FR, SE, and AHP respectively. The marginal but consistent improvement in AUC from training to validation datasets confirmed the absence of overfitting and strong generalization capability across all approaches. The convergence of results across three fundamentally different methodologies strengthens the scientific credibility of the produced susceptibility maps, establishing them as reliable and practically applicable tools for disaster risk reduction, slope stabilization prioritization, and informed land-use planning in landslide-prone Himalayan regions.

CHAPTER 6

LIMITATION AND FUTURE FOCUS

- Firstly, the investigation considered ten only factors that influence landslides, however, some very important aspects were left out such as soil type, changes in land use and land cover, and rainfall intensity. The omission of these aspects may have reduced the completeness of the susceptibility assessment.
- The landslide inventory of 366 events represents a static single-temporal dataset and does not capture the evolving nature of landslide occurrence under changing climatic and land-use conditions over time.
- The AHP model relies on expert judgment for pairwise comparisons, introducing an inherent element of subjectivity that, despite the acceptable Consistency Ratio of 0.008, cannot be entirely eliminated from the weighting process.
- Advanced machine learning algorithms such as Random Forest, Support Vector Machine, and Gradient Boosting should be integrated and compared against the three models applied in this study to further improve predictive accuracy in this complex Himalayan terrain.
- Multi-temporal landslide inventories derived from repeat satellite imagery and SAR interferometry should be developed to monitor and dynamically update susceptibility assessments in response to evolving climatic and land-use conditions.
- A comprehensive hazard and risk assessment framework should be established by coupling the produced susceptibility maps with rainfall threshold analysis, population vulnerability data, and critical infrastructure exposure, ultimately supporting the development of real-time early warning systems for Pithoragarh District.

Pithoragarh District Uttarakhand

ORIGINALITY REPORT

9%	3%	9%	0%
SIMILARITY INDEX	INTERNET SOURCES	PUBLICATIONS	STUDENT PAPERS

PRIMARY SOURCES

1	"Climate Change, Environmental Hazards and Community-Based Resilience", Springer Science and Business Media LLC, 2026 Publication	1%
2	"Geomorphic Risk Reduction Using Geospatial Methods and Tools", Springer Science and Business Media LLC, 2024 Publication	1%
3	Brototi Biswas, Bhagwan Ghute, Jayanta Das. "Geoinformatics for Flood Risk Management - Applications and Strategies", CRC Press, 2025 Publication	1%
4	Jyoti Yadav, Rajesh Kumar Dash, Debi Prasanna Kanungo. "Spatial prediction of landslides in Pithoragarh district, Kumaon Himalaya, India", Journal of Earth System Science, 2025 Publication	<1%
5	Rukhsana Sarkar, Asraful Alam, Azizur Rahman Siddiqui. "Agriculture and Climatic Issues in South Asia - Geospatial Applications", CRC Press, 2023 Publication	<1%
6	Mohammed Alghamdi, Salman Alhifthi, Naif Alsanabani, Khalid Al-Gahtani, Ayman Altuwaim, Abdullah AlSharef. "Modeling the interdependencies of critical factors in hospital facility management: a system	<1%

dynamics framework", Ain Shams Engineering Journal, 2026
Publication

7	Pooja Rana, Jeganathan Chockalingam, Arvind Chandra Pandey. "chapter 7 Space-Time Integrated Landslide Hazard Zonation near Tehri Dam in Uttarakhand, India", IGI Global, 2017 Publication	<1 %
8	Yasser M. Khalil, Yousef A. Al-Masnay, Nabil M. Al-Areeq, Ali R. Al-Aizari, Bazel Al-Shaibah, Xingpeng Liu. "Estimating landslide hazard distribution based on machine learning and bivariate statistics in Utmah Region, Yemen", Natural Hazards, 2023 Publication	<1 %
9	www.hindawi.com Internet Source	<1 %
10	Mustapha Ait Omar, Issam Etebaai, Morad Taher, Abdelhamid Tawfik. "Landslide susceptibility mapping in the Bokoya Massif, Northern Morocco: A geospatial and multi-factor analysis using the analytic hierarchy process (AHP)", Scientific African, 2025 Publication	<1 %
11	"Impact of Climate Change, Land Use and Land Cover, and Socio-economic Dynamics on Landslides", Springer Science and Business Media LLC, 2022 Publication	<1 %
12	Kaiwan K. Fatah, Yaseen T. Mustafa, Imaddadin O. Hassan. "Geoinformatics-based frequency ratio, analytic hierarchy process and hybrid models for landslide susceptibility zonation in Kurdistan Region, Northern Iraq",	<1 %

Environment, Development and Sustainability, 2023
Publication

13	"Engineering Geology for Society and Territory - Volume 2", Springer Nature, 2015 Publication	<1 %
14	Duc-Dam Nguyen, Quynh-Anh Thi Bui, Hiep Van Le, Binh Thai Pham et al. "Landslide Susceptibility Mapping Using RBFN-Based Ensemble Machine Learning Models", Computer Modeling in Engineering & Sciences, 2025 Publication	<1 %
15	Janaki Ballav Swain, Ningthoujam James Singh, Lovi Raj Gupta. "Landslide susceptibility zonation of a hilly region: A quantitative approach", Natural Hazards Research, 2023 Publication	<1 %
16	Naveen Chandra, Elizabath, Swapnamita Choudhury, Himadri Vaidya. "Integrated Spatial Landslide Risk Assessment for Population and Infrastructure in Tehri, Garhwal Himalayas, India", Geological Journal, 2026 Publication	<1 %
17	www.co.knox.oh.us Internet Source	<1 %
18	Selemon Thomas Fakana, Fekadu Fanjana Falta, Megegn Mada Mano, Elias Bojago, Mekonen Shibru Gebremariam, Mathewos Markos Fakana. "Mapping landslide susceptibility in Wolaita Zone, Ethiopia, using geospatial techniques and multi-criteria decision-making analysis", Journal of African Earth Sciences, 2026 Publication	<1 %

19	Chuan Zhang, Muhammad Akhlaq, Haofang Yan, Yuxin Ni, Shaowei Liang, Junan Zhou, Run Xue, Min Li, Rana Muhammad Adnan, Jun Li. "Chlorophyll fluorescence parameter as a predictor of tomato growth and yield under CO2 enrichment in protective cultivation", Agricultural Water Management, 2023 Publication	<1 %
20	Tekendra Bahadur Saud, Prakash Bahadur Ayer, Mahesh Prasad Awasthi, Bharat Prasad Bhandari, Narayan Raj Joshi. "Application of bivariate frequency ratio and information value models for landslide susceptibility in Thuligad watershed of far-western Nepal", Discover Geoscience, 2025 Publication	<1 %
21	link.springer.com Internet Source	<1 %
22	"Urban Blue-Green Infrastructure Approach for Food Security and Climate Disaster Resilience", Springer Science and Business Media LLC, 2025 Publication	<1 %
23	Alemnew Ali, Degfie Teku, Tesfaldet Sisay, Bishaw Mihret. "A combined analysis of frequency ratio and analytical hierarchy process for landslide susceptibility assessment in Tenta, South Wollo, Ethiopia", Scientific Reports, 2025 Publication	<1 %
24	Ambikesh Dwivedi, Amarnath Hegde. "Hybrid Approach for Landslide Susceptibility Mapping and Socio-Economic Landslide Risk Assessment in Meghalaya, India", Progress in Engineering Science, 2026 Publication	<1 %

25	Engdaw Gulbet, Belete Getahun. "LANDSLIDE SUSCEPTIBILITY MAPPING USING FREQUENCY RATIO AND ANALYTICAL HIERARCH PROCESS METHOD IN AWABEL WOREDA, ETHIOPIA", Quaternary Science Advances, 2024 Publication	<1 %
26	Andang Suryana Soma, Tetsuya Kubota, Hideaki Mizuno. "Optimization of causative factors using logistic regression and artificial neural network models for landslide susceptibility assessment in Ujung Loe Watershed, South Sulawesi Indonesia", Journal of Mountain Science, 2019 Publication	<1 %
27	Imran Khan, Harish Bahuguna, Ashutosh Kainthola, Rayees Ahmed, Md. Sarfaraz Asgher. "National-scale landslide susceptibility and risk mapping of India using a hybrid data-driven approach", Scientific Reports, 2025 Publication	<1 %
28	Shubham Singh, Nirlipta Priyadarshini Nayak, Ashish Aggarwal, Harsh Kumar Verma. "Role of remote sensing and geotechnical studies in assessing the landslide vulnerability in the Chamoli region of Uttarakhand, India", Discover Applied Sciences, 2025 Publication	<1 %
29	Tadele Melese, Tatek Belay, Azene Andemo. "Application of analytical hierarchal process, frequency ratio, and Shannon entropy approaches for landslide susceptibility mapping using geospatial technology: The case of Dejen district, Ethiopia", Arabian Journal of Geosciences, 2022 Publication	<1 %

30	etd.aau.edu.et Internet Source	<1 %
31	www.researchgate.net Internet Source	<1 %
32	Devraj Dhakal, Kanwarpreet Singh, Damandeep Kaur, Sahil Verma et al. "Landslide-induced vulnerability of road networks in Lahaul and Spiti, India: a geospatial study", Bulletin of Engineering Geology and the Environment, 2025 Publication	<1 %
33	ir.lib.nycu.edu.tw Internet Source	<1 %
34	pmc.ncbi.nlm.nih.gov Internet Source	<1 %
35	Ambikesh Dwivedi, Surya Sarat Chandra Congress, Raul Velasquez, Prince Kumar, Ujwalkumar Patil. "Explainable AI (xAI) for Landslide Susceptibility Modeling: A Comparative Analysis of Machine Learning and Deep Learning Approaches", Earth Systems and Environment, 2026 Publication	<1 %
36	Meenakshi Devi, Anand Kumar Gupta, Chan-Young Yune, Bikash Kumar Ram. "Preliminary inferences on the August 5, 2025, catastrophic debris flow in Dharali, India: insights from the satellite imageries and geomorphological analysis of the Kheer Gad watershed", Landslides, 2026 Publication	<1 %
37	Suman Kanungo, Ranjan Kumar Nandy, Rounik Talukdar, Manoj Murhekar et al. "Analysis of Cholera Risk in India: Insights from 2017–18 Serosurvey Data Integrated	<1 %

with Epidemiologic data and Societal Determinants from 2015–2019", PLOS Neglected Tropical Diseases, 2024
Publication

38	paperswithcode.com Internet Source	<1 %

Exclude quotes	Off	Exclude matches	< 14 words
Exclude bibliography	Off		

Pithoragarh District Uttarakhand

GRADEMARK REPORT

FINAL GRADE

/0

GENERAL COMMENTS

PAGE 1

PAGE 2

PAGE 3

PAGE 4

PAGE 5

PAGE 6

PAGE 7

PAGE 8

PAGE 9

PAGE 10

PAGE 11

PAGE 12

PAGE 13

PAGE 14

PAGE 15

PAGE 16

PAGE 17

PAGE 18

PAGE 19

PAGE 20

PAGE 21

PAGE 22

PAGE 23

PAGE 24

PAGE 25

PAGE 26

PAGE 27

PAGE 28

PAGE 29

PAGE 30

PAGE 31

PAGE 32

PAGE 33

PAGE 34

PAGE 35

PAGE 36

PAGE 37

PAGE 38

PAGE 39

PAGE 40

PAGE 41

PAGE 42

PAGE 43

PAGE 44

PAGE 45

PAGE 46

PAGE 47

PAGE 48

PAGE 49

PAGE 50

PAGE 51

PAGE 52

PAGE 53